International Journal of Modern Physics E, Vol. 7, No. 4 (August 1998) 527–551

CLASSICAL AND QUANTAL CHAOS DESCRIBED BY A FOURTH ORDER QUADRUPOLE BOSON HAMILTONIAN

V. BARAN and A. A. RADUTA
Institute of Physics and Nuclear Engineering,
PO Box MG-6,
R-76900 Bucuresti-Magurele, Romania

Received 6 October 1997

A quadrupole boson Hamiltonian is considered within a time dependent variational formalism. The trial functions are coherent states with respect to the quadrupole bosons b_0^+ and $b_2^+ + b_{-2}^+$. The character, chaotic or regular, of the classical trajectories are studied, in terms of both the Poincaré surface of sections and maximal Lyapunov exponents, as a function of energy and an order parameter B, the coefficient of the third order boson term. A peculiar feature concerning the behavior of chaos and order in the range of large energies is pointed out. Quantizing the classical energy function one obtains an operator whose spectrum is analyzed in terms of level spacing distribution. Some classical and quantal features of the chaotic motion are possibly related.

1. Introduction

Some properties of a non-integrable Hamiltonian obtained by perturbing, with H_1, an integrable Hamiltonian function might be interpreted within the framework of Kolmogorov-Arnold-Moser theorem:[1] if the perturbation is 'small enough' the phase-space tori of the unperturbed system will survive by being deformed. However some of 'rational tori', i.e, tori characterized by a rational ratio of characteristic frequencies, say r/s, are destroyed under the H_1 action and there by the emptied region of the phase space may be occupied by trajectories having chaotic behavior. There are, however, an even number of fixed points, half stable and half unstable, which survive. Rigorously speaking, not only the above mentioned tori disappear but all those whose frequency ratios are in a sphere centered in r/s and having a radius $K/s^{2.5}$, K being a function which goes to zero when H_1 tends to zero.[8] All these properties constitute generic features for non-integrable systems.

Moreover, the numerical analysis for various systems showed that some tori are preserved even for strong perturbative terms although one notices the onset and the development of the so-called "widespread chaos". The mechanism which causes this phenomenon is the resonances overlap.[2] Indeed, the perturbation can always be written as a Fourier series of angle variables associated to the integrable Hamiltonian, the expansion coefficients being functions of actions. Each term of

this expansion defines a resonance which is acting in a certain region D_r of the phase space, where the chosen term is non-vanishing. A resonance is called isolated if the corresponding domain D_r is not intersected by any of the remaining D_k. If a tori intersects D_r, it will be distorted by the isolated resonance but not destroyed. However, if there are two resonances whose substrate D_1 and D_2 intersect each other, they destroy any tori of the integrable Hamiltonian, which goes through the intersection domain of D_1 and D_2. Consequently the onset of a chaotic motion is generated. In this context we mention the work of Walker and Ford,[3] where the non-integrable part consists of two terms yielding the resonances 2:2 and 3:2, respectively. The authors concluded that by increasing the system's energy, a critical value is met when the two resonances start overlapping with each other and the widespread chaos is suddenly settled. Until that critical energy is reached, the isolated resonances produce only a distortion of the tori in the associated phase space volume.

An interesting connection between dynamical symmetry breaking for the given quantum Hamiltonian and the onset of chaos in the corresponding classical system was established in Refs. 4, 5. The farther the system is from the dynamical symmetry, the more involved the chaos onset is.

The link between the chaotic/regular features of classical orbits and the quantum mechanical spectrum was suggested by Percival in Ref. 6. The irregular quantal states have the specific property that are more sensitive to a slowly changing perturbation than a regular state. An alternative definition, in terms of the corresponding eigenvectors, was given in Ref. 7 by making use of the semiclassical periodic theory.[8] The quantitative analysis of chaotic quantal motions is usually made in terms of the random matrix theory.[9] Thus the spectra of realistic Hamiltonians used in various fields of physics[3,10–15] have been studied. Surprisingly, many of them display a nearest neighbor spacing (NNS) distribution which is characteristic of the Gaussian orthogonal ensemble (GOE or Wigner distribution).[16]

In nuclear physics the subject became very popular since two sets of experimental data concerning neutron resonance states[17] and low lying collective states[18] were analysed. Thus, in Ref. 17 it was shown that the spacing distribution for neutron resonance states is very well reproduced by a Wigner distribution. Concerning the collective levels of a given spin and parity,[18] they satisfy a regular (Poisson) statistics when J^π is equal to $2^+, 4^+$ respectively, while for $0^+, 3^+$ the spacing statistic is closer to GOE. A strong mass dependence of nuclear spectra was pointed out in Ref. 19. Thus the lightest nuclides show a behavior close to GOE while the heaviest ones display a Poisson behavior. These pioneering papers were followed by many theoretical works aimed at seeking the degree of chaos of nuclear states exhibiting a certain symmetry. Investigations were made within microscopic,[9,20–27] phenomenological,[29–32] and semimicroscopic formalisms,[33–35] respectively. Fluctuation properties of nuclear spectra have been obtained by calculating either of the statistics: NNS, Δ_3 (this is a measure for the deviation from equal spacing[36] and is conventionally called spectral rigidity), $\Sigma^2(r)$ (the variance of the level number

in an interval of length r). The predictions are compared with one of the reference Poisson statistics (Wigner and Brody[9]). The departure from the regular distribution is usually attributed to a certain parameter of the model Hamiltonian whose magnitude decides a specific symmetry breaking or the strength of the coupling between different degrees of freedom.

In a recent publication we investigated the chaotic behavior of a nuclear system, described in terms of quadrupole bosons, and concluded that this changes whenever a phase transition takes place. In other words, chaos carries the fingerprints of the nuclear phase.[37]

The aim of this paper is to continue the study of a certain phase of the nuclear system mentioned above and show that the volume of phase space occupied by regular orbits is enlarged by increasing the system energy. If the energy is further increased, chaos prevails again. Some straight consequences of such a behavior are commented. The chaotic features of the classical motion in a restricted energy interval are reflected in the spectrum structure of the quantal operator obtained from the classical energy function through a quantization procedure. This analysis will be developed according to the following plan. In Sec. 2 the model Hamiltonian is presented. Also the notations as well as the necessary conventions are fixed. Section 3 is devoted to the classical trajectories in the phase space. The partition of the phase space in two volumes occupied by regular and chaotic trajectories respectively, is pictorially shown by means of the Poincaré surface of sections. The specific properties for a chaotic volume at a fixed energy are quantified by calculating the largest Lyapunov exponent. A possible explanation of these classical features is made in terms of the KAM theorem and the overlapping resonances mechanism. In Sec. 4, the probability distributions of the quantized Hamiltonian eigenvalues are given. Possible relations between the classical and quantal chaotic features are discussed. Final conclusions are drawn in Sec. 5.

2. The Model Hamiltonian

Since the present work continues the investigations of two earlier publications[37,38] we borrow from there the quadrupole boson Hamiltonian

$$H = A_1[b^+b]_0 + \Big\{A_3([b^+b^+]_0 + [b^+b^+b^+]_0 + 3[b^+b^+b]_0) + A_4\Big(\frac{1}{4}[b^+b^+]_0[b^+b^+]_0 + [b^+b^+]_0[b^+b]_0\Big) + H.c.\Big\} + A_4\left(\frac{1}{2}[b^+b^+]_0[bb]_0 + \overbrace{[b^+\underbrace{[b^+b]}_{0}b]}^{0}\right). \tag{2.1}$$

In terms of quadrupole coordinates and conjugate momenta,

$$\alpha_\mu = \frac{1}{\sqrt{2}}(b^+_\mu + (-)^\mu b_{-\mu}), \quad \pi_\mu = \frac{i}{\sqrt{2}}((-)^\mu b^+_{-\mu} - b_\mu), \quad -2 \le \mu \le 2, \tag{2.2}$$

the model Hamiltonian acquires a simple expression

$$H = \mathcal{A} + \mathcal{B}(\pi\pi)_0 + \mathcal{C}(\alpha\alpha)_0 + \mathcal{D}_3(\alpha\alpha\alpha)_0 + \mathcal{D}_4(\alpha\alpha)_0(\alpha\alpha)_0\,, \tag{2.3}$$

which exhibits the particular feature that momenta are not coupled with coordinates and moreover the terms of fourth order in momenta are missing. This type of Hamiltonian was extensively used by the Frankfurt group[39] to describe the spectroscopic properties of rotational bands in heavy nuclei. As considered in Ref. 40, the most realistic Hamiltonian is that which includes all fourth order boson terms. The Hamiltonian 2.1 has, however, the advantage that despite its small number of parameters, it is able to describe all known nuclear phases. Moreover this Hamiltonian contains a parameter B, proportional to A_3, which plays the role of an "order" parameter. Indeed for $B = 0$ the classical system, associated to H, is integrable and the corresponding trajectories are regular, while for $B \neq 0$ the chaotic trajectories may appear. Due to these properties H suits the scope of the present paper.

The coefficients $\mathcal{A}$, $\mathcal{B}$, $\mathcal{C}$, $\mathcal{D}_3$, $\mathcal{D}_4$ are related to those defining the boson Hamiltonian by simple equations, which were given in Ref. 37. Without losing the generality, in this paper we shall use a boson representation where $A_2 = 0$.

This Hamiltonian will be studied through a time dependent variational principle (TDVP)[a]:

$$\delta \int_0^t \left\langle \psi | H - i\frac{\partial}{\partial t'} | \psi \right\rangle dt' = 0 \tag{2.4}$$

where the variational space is spanned by a coherent state

$$|\psi\rangle = \exp[z_0 b_0^+ - z_0^* b_0 + z_2(b_2^+ + b_{-2}^+) - z_2^*(b_2 + b_{-2})]|0\rangle\,, \tag{2.5}$$

which depends on two time dependent complex parameters, z_0, z_2. Denoting by

$$q_k = 2^{\frac{2+k}{4}}\,\mathrm{Re}(z_k)\,, \quad p_k = 2^{\frac{2+k}{4}}\,\mathrm{Im}(z_k)\,, \quad k = 0, 2\,. \tag{2.6}$$

Equation (2.4) provides, for the variables (q_k, p_k), a set of classical equations of Hamilton type

$$\dot{q}_k = \frac{\partial \mathcal{H}}{\partial p_k}\,,$$

$$\dot{p}_k = -\frac{\partial \mathcal{H}}{\partial q_k}\,, \quad k = 0, 2 \tag{2.7}$$

with $\mathcal{H}$ denoting the average value of H on the variational state 2.5:

$$\mathcal{H}(q_0, p_0, q_2, p_2) = \frac{A}{2}(p_0^2 + p_2^2 + q_0^2 + q_2^2) + \frac{B}{\sqrt{2}} q_0(3q_2^2 - q_0^2) + \frac{D}{4}(q_0^2 + q_2^2)^2\,. \tag{2.8}$$

[a] Hereafter the units $\hbar = 1$ will be used.

This has the meaning of a classical Hamiltonian describing the motion of two degrees of freedom in the phase space of coordinates $(q_0, p_0; q_2, p_2)$. The coefficients A, B, D are related to those involved in Eq. (2.1) by:

$$A = \frac{1}{\sqrt{5}} A_1 , \quad B = \frac{16}{\sqrt{35}} A_3 , \quad D = \frac{5}{4} A_4 . \tag{2.9}$$

As shown in Ref. 37, $\mathcal{H}$ is a sum of two terms, one of integrable

$$H_0(q_0, p_0, q_2, p_2) = \frac{A}{2}\left(p_0^2 + p_2^2 + q_0^2 + q_2^2\right) + \frac{D}{4}\left(q_0^2 + q_2^2\right)^2 , \tag{2.10}$$

and one of non-integrable type

$$H_1(q_0, p_0, q_2, p_2) = \frac{B}{\sqrt{2}} q_0\left(3q_2^2 - q_0^2\right) . \tag{2.11}$$

Indeed, in the former case there are two well-defined constants of motion, namely H_0 and

$$\Phi_\gamma = \frac{1}{2}(q_0 p_2 - q_2 p_0) . \tag{2.12}$$

The fact that Φ_γ is a constant of motion reflects the invariance of H against any rotation T_3 around an axis perpendicular on the (q_0, q_2) plane

$$[H, T_3] = 0 , \quad T_3 = \frac{1}{2i\sqrt{2}} \left[b_0^\dagger (b_2 + b_{-2}) - \left(b_2^\dagger + b_{-2}^\dagger\right) b_0 \right] . \tag{2.13}$$

The operators T_3 and

$$\begin{aligned} T_1 &= \frac{1}{4} \left[2 b_0^+ b_0 - \left(b_2^\dagger + b_{-2}^\dagger\right)\left(b_2 + b_{-2}\right) \right] , \\ T_2 &= \frac{1}{2\sqrt{2}} \left[b_0^\dagger (b_2 + b_{-2}) + \left(b_2^\dagger + b_{-2}^\dagger\right) b_0 \right] , \end{aligned} \tag{2.14}$$

generate a rotation group Re acting in a fictitious space. It can be easily checked that Φ_γ is the expected value of T_3 in the state ψ given by Eq. (2.5).

When $B \neq 0$, the Hamiltonian $\mathcal{H}$ can be viewed as a sum of a Hamiltonian of Henon–Heiles type and a term of fourth degree in coordinates. For this case, Φ_γ is no longer a well defined constant of motion. Moreover, besides $\mathcal{H}$ there is no other constant of motion. Indeed, according to Ref. 41 the Henon–Heiles Hamiltonian is not integrable.

The classical properties of H were studied in Ref. 38. The chaotic versus regular features of classical trajectories were described, for various sets of energy and "ordering parameter" B, in terms of the Poincaré surface of sections and maximal Lyapunov coefficients.[37] The analysis was performed for all "nuclear phases" defined by particular choices of the parameters involved in the model Hamiltonian.

Additional properties of the classical chaotic motion will be presented in the next section. Moreover, the classical chaos associated to a given nuclear phase will be related to a specific behavior of the spectrum of the quantal boson Hamiltonian

$$
\begin{aligned}
H_B = {} & A\left(a_0^\dagger a_0 + a_2^\dagger a_2\right) + \frac{B}{4}\left[\left(3a_0^\dagger {a_2^\dagger}^2 + 3a_0 a_2^2 - {a_0^\dagger}^3 - a_0^3\right)\right. \\
& \left. + 3\left({a_2^\dagger}^2 a_0 + a_0^\dagger a_2^2 - a_0^\dagger a_0^2 - {a_0^\dagger}^2 a_0 + 2a_2^\dagger a_2 a_0 + 2a_2^\dagger a_2 a_0^\dagger\right)\right] \\
& + \frac{D}{16}\left[6\left({a_0^\dagger}^2 a_0^2 + {a_2^\dagger}^2 a_2^2\right) + 2\left({a_0^\dagger}^2 a_2^2 + {a_2^\dagger}^2 {a_0}^2\right) + 8a_0^\dagger a_2^\dagger a_0 a_2\right. \\
& + 4\left(a_0^\dagger a_0^3 + {a_0^\dagger}^3 a_0 + a_2^\dagger a_2^3 + {a_2^\dagger}^3 a_2 + a_2^\dagger a_2 a_0^2 + a_2^\dagger a_2 {a_0^\dagger}^2 + a_0^\dagger a_0 a_2^2 + a_0^\dagger a_0 a_2^2\right) \\
& \left. + \left({a_0^\dagger}^4 + a_0^4 + {a_2^\dagger}^4 + a_2^4 + 2{a_0^\dagger}^2 {a_0^\dagger}^2 + 2a_0^2 a_2^2\right)\right] \qquad (2.15)
\end{aligned}
$$

obtained from $\mathcal{H}$ through the quantization transformation

$$
\begin{aligned}
& q_k \to \hat{q}_k\,, \quad p_k \to \hat{p}_k = -i\hbar\frac{\partial}{\partial q_k}\,, \\
& \hat{q}_k = \frac{1}{\sqrt{2}}\left(a_k^\dagger + a_k\right), \quad \hat{p}_k = \frac{i}{\sqrt{2}}\left(a_k^\dagger - a_k\right). \qquad (2.16)
\end{aligned}
$$

Using the transformations given by the first row of the above equations and then the polar coordinates for the (q_0, q_2) plane one easily obtains an alternative expression for the quantized Hamiltonian:

$$
H_B = -\frac{A}{2}\left(\frac{\partial^2}{\partial r^2} + \frac{1}{r}\frac{\partial}{\partial r} + \frac{1}{r^2}\frac{\partial^2}{\partial\theta^2}\right) + \frac{A}{2}r^2 - \frac{B}{\sqrt{2}}r^3\cos 3\theta + \frac{D}{4}r^4\,. \qquad (2.17)
$$

To obtain the eigenvalues of the quantized Hamiltonian, we have diagonalized H_B, given by Eq. (2.16), in a basis constructed by acting with the operators ${a_0^\dagger}^{n_1}{a_2^\dagger}^{n_2}$ on the boson vacuum state, $|0\rangle$. Replacing $b_0^\dagger, b_0$ and $\frac{1}{\sqrt{2}}(b_2^\dagger + b_{-2}^\dagger)$, $\frac{1}{\sqrt{2}}(b_2 + b_{-2})$ by $a_0^\dagger$, a_0 and $a_2^\dagger$, a_2, respectively, in the equations of T_k, $k = 1, 2, 3$ one obtain the generators of a rotation group acting in the $a_0^\dagger, a_2^\dagger$ boson space. The *irrep* of the new $\mathfrak{R}_3$ group can be alternatively used to study the eigenstates of H_B. If H_B exhibits invariance properties with respect to either $\mathfrak{R}_3$ or one of its subgroups, its eigenstates can be classified by the eigenvalues of the Casimir operators associated with these groups. When the rotational degrees of freedom are switched on, a full rotational band can be constructed on top of each energy level characterizing H_B. One should stress the fact that the procedure mentioned above provides a new classification of rotational bands which contrasts with the traditional one given by Bohr and Mottelson.[42]

Before closing this section we would like to summarize the main results. If the variational state $|\psi\rangle$ would be a product of 5 coherent states corresponding to the

5 boson components respectively, then solving the equations provided by the variational principle would be equivalent to solving the Schrodinger equation associated to H. By restricting the states to those given by (2.5) only a certain class of states can be described. Indeed, the classical equations describe two degrees of freedom (out of five), which, as we proved in Ref. 38, could be identified with the dynamic deformation variables β and γ. Suppose now that H can be separated into three pieces: one describing the intrinsic motion, one describing the rotational motion and one the coupling term. The first operator can be mapped with H_B. In this way the spectrum of H_B consists of energy levels of a coupled system of two intrinsic degrees of freedom. In order to fully characterize the spectrum of H it is necessary to account for the motion of the rotational degrees of freedom. In conclusion we deal with the classical and quantal motion of the "intrinsic" coordinates q_0, q_2 which, according to Ref. 38, can be related to the nuclear dynamic deformations β and γ.

3. Some Remarks on the Chaotic Behavior of $\mathcal{H}$

In this section we focus our attention on classical trajectories determined by the Eq. (2.7) with B chosen such that H_1 may be considered as a perturbation comparing it with H_0. As we have already mentioned, the perturbative term is similar to that considered in the Henon–Heiles Hamiltonian.[41] In contrast, the integrable part of our Hamiltonian comprises a term which is of fourth order in coordinates and therefore for any energy, the trajectories are confined in a bounded volume of the coordinates space. The surface potential energy has only one minimum, in origin, if the parameter B obeys the relation:

$$9B^2 - 8AD \leq 0\,. \tag{3.1}$$

In what follows we shall consider only those values of B satisfying the above inequality. Without losing generality of the final results we take the parameters B as given by (3.1), $D = 0.4$ A (fixed), and energy values in units of A. Under these circumstances, the time unit is necessarily equal to $\frac{\hbar}{A}$.

The classical equations of motion (2.7) were integrated by the fourth order Runge-Kutta method resulting in an integration relative error, for the energy conservation, smaller than 0.5 per cents. Using the Poincaré surface of section method,[49] we investigated the change in the phase space structure (i.e. we explored the volumes scanned by chaotic and regular trajectories, respectively), when energy varies in a very large interval. Let us consider a value for the parameter B lying 'far' from that corresponding to the integrability case (the meaning of this statement will become clear later). For $B = 0.55$ A, in Fig. 1 we have plotted the Poincaré sections in the plane (u_2, v_2) at energies $E = 5$ A MeV, 30 A MeV, 120 A MeV, 240 A MeV, 400 A MeV, 600 A and 1000 A MeV, respectively. The remaining coordinates are fixed by the restrictions:

$$u_0 = 0\,, \quad v_0 \geq 0\,, \quad \mathcal{H} = E\,. \tag{3.2}$$

From Fig. 1 one sees that at low energy widespread chaos is installed in a large volume. Even for larger energy, such as 30 A (MeV), only few 'regular' islands are filled by tori. However when the energy is increased, other regular regions are generated and the relative volume occupied by chaotic orbits becomes smaller and smaller. The regular region for $E = 240$ A MeV is larger than those corresponding to the former energies. The limiting case is obtained for $E = 400$ A (MeV) when the phase space is fully occupied by tori. A similar structure is seen at 600 A (MeV) but the separatrix is simpler. A natural question arises: why is the widespread chaos

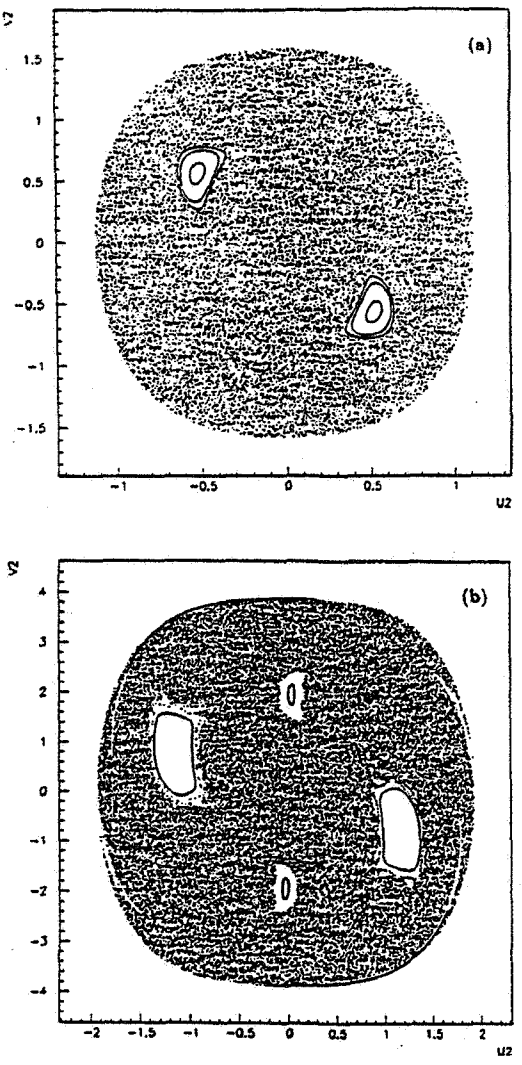

Fig. 1. (a) The Poincaré surface of section for $B = 0.55$ A (MeV) and an energy E equal to a 5 A (MeV), (b) 30 A (MeV), (c) 120 A (MeV), (d) 240 A (MeV), (e) 400 A (MeV), (f) 600 A (MeV), (g) 1000 A (MeV), (h) For $B = 0.55$ A (MeV) the largest Lyapunov exponent is plotted as a fuction of energy.

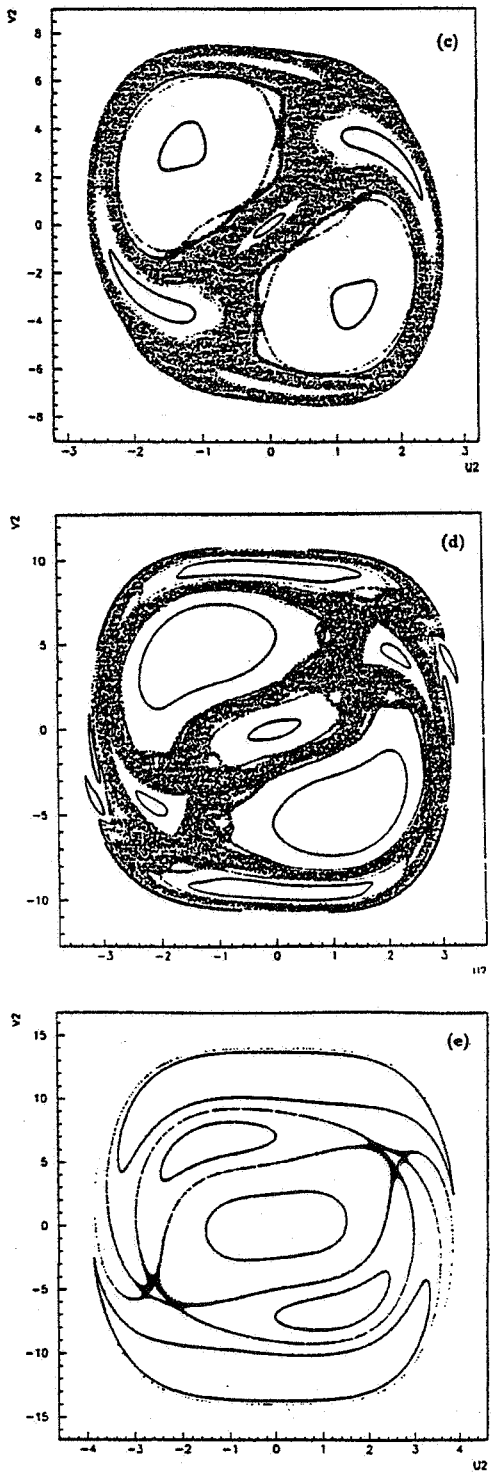

Fig. 1. (*Continued*)

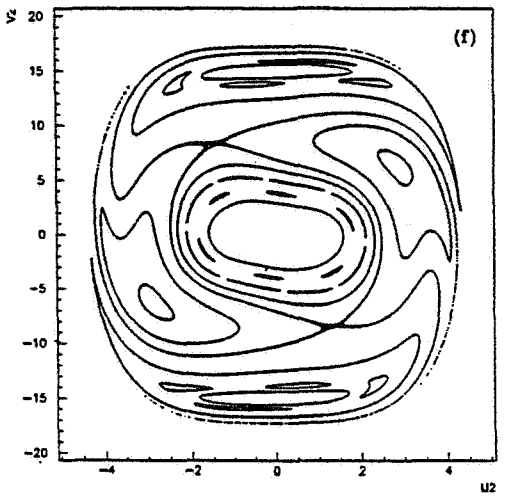

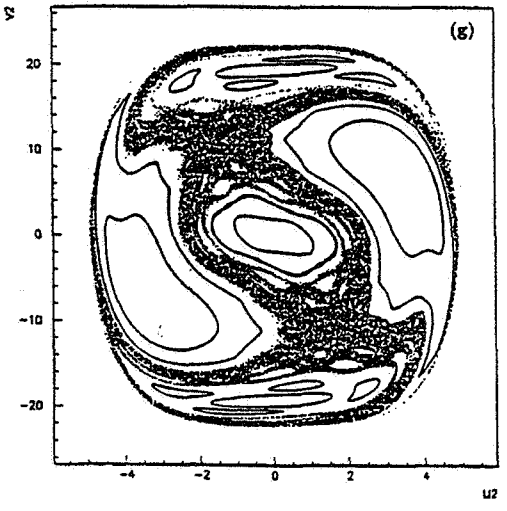

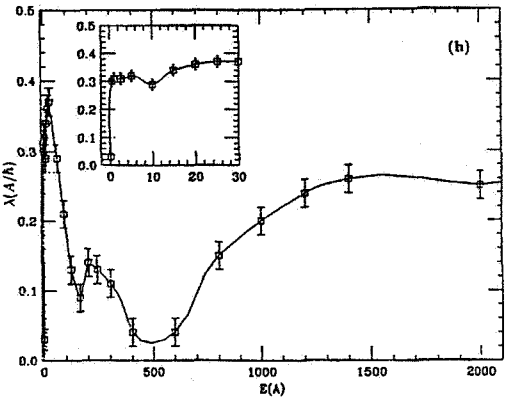

Fig. 1. (*Continued*)

suppressed by increasing the energy? This is because by increasing the system energy, the integrable part, due to the term of fourth order in coordinates, prevails over the non-integrable one, which is only of third order. Moreover, since the perturbation is weaker, when one increases the energy, the resonances have a smaller overlap or even ceases to overlap.

However, at a higher energy (1000 A MeV) a new behavior shows up: a chaotic volume appears again in the region of separatrices delimiting the tori surrounding different elliptical points. It turns out that this structure remains almost unchanged over a very large range of energy. Thus, a similar Poincaré surface of section is also detected at an energy of 10^4 A MeV. However after a flat maximum is reached, there is a slight tendency to decrease the relative chaotic volume when the system energy is increased.

The appearance of chaos, when the energy is increased beyond the value of 600 A (MeV), happened when new resonances are suddenly switched on and these overlap the ones which already showed up at lower energy. Indeed, if only one resonance was effective in the region where the chaos is now settled, tori from the preceding picture would have survived after the perturbation was switched on. An example of such a sharp onset of a new resonance is analyzed in Ref. 3. We would like to stress on that the oscillating behaviour of both classical and quantal systems from chaos to order and again to chaos is not a result of the competition between the third and fourth order boson terms, as one might think at a superficial glance. Indeed, the invoked argument would justify the first transition from a chaotic to a regular regime but, by no means, could not explain the onset of widespread chaos when the energy is further increased. To conclude, our model points out a new feature concerning the competition between chaos and regular motion in sharing the phase space volume. Indeed, for the first time an oscillating-like behavior, from chaos to order and from order again to chaos, of the motion character is shown when the total energy increases. It is worth mentioning that the features presented in Figs. 1(a)–(g) are more or less conserved when we change the section, i.e. the first restriction from Eq. (3.2). This makes us believe that the ratio of the chaotic and regular volumes of the phase space exhibits a similar trend as the ratio of the corresponding areas in the Poincaré sections shown here. It is worth noting here that the third order Hamiltonian in (2.8) (for the case $D = 0$) is associated to a starting quadrupole boson Hamiltonian, which is widely used to describe a certain class of collective properties of nuclear systems while, a long time ago, it was used to explore the galaxies of motion. This fact encourages us to hope that although beyond the interval [0, 30] A (MeV) we use "unphysical" energies for nuclear surface oscillations,[43] the new unveiled features are interesting not only in themselves but also for the perspective of describing other systems which accommodate energies lying in this range. However to get definite relevance for nuclear system we focus our attention on the correspondence between classical and quantal chaos, within the interval of [0, 30] A (MeV). As we shall see, later, large deviations from what is commonly known are pointed out.

We quantify the qualitative results presented above by plotting (see Fig. 1(h)) the energy dependence of the largest Lyapunov exponent (LE). The LE is calculated according to the standard definition:

$$\lambda = \lim_{t\to\infty} \frac{1}{t} \ln \frac{D(t)}{D(0)} \tag{3.3}$$

where $D(t)$ is the distance, at time t, between two neighboring trajectories chosen such that at the initial time ($t = 0$) they were apart by a given small distance $D(0)$. In order to avoid the errors induced by the square operation we make the option for the following norm definition in the phase space:[44]

$$D = \sum_{i=0,2} \left\{ \left| q_i^{(1)} - q_i^{(2)} \right| + \left| p_i^{(1)} - p_i^{(2)} \right| \right\} . \tag{3.4}$$

One should mention that the final result does not depend on the particular choice of the norm definition. Since the chosen system has two degrees of freedom this has only two non-vanishing Lyapunov exponents, which are of equal magnitudes but of different signs. In order to calculate the limit involved in the defining Eq. (3.3) we have used the method of Bennetin and Galgani in Ref. 45. The results reported here correspond to an initial distance of the order $D(0) = 10^{-6}$ and a time interval for two successive renormalization of about $\Delta\tau = 80$.

To test the procedure employed, we calculated successively the Lyapunov exponent for a harmonic oscillator and the integrable system obtained for $B = 0$. In both cases we got for λ a value smaller than 0.04. Clearly this value might be considered as a measure for the error order of magnitude, even for more complex situations. Indeed, similar results for λ are obtained in the regular region of the non-integrable system, irrespective of the energy value. Also, it is worth mentioning that the reported values for the largest Lyapunov exponent depend neither on initial conditions nor the $\Delta\tau$ values. This statement is valid for large intervals of $D(0)$ and $\Delta\tau$, respectively.

The convergence properties of the limit (3.3) were checked by considering a large number of initial conditions defining trajectories of chaotic and regular types, respectively. It is fair to say that we did not meet situations when this limit does not exist. As a matter of fact this result agrees entirely with the numerical analysis described by Henon in Ref. 46. The reason is that in both cases, here and there, the conditions for Osedelec[48] theorem are fulfilled.[49]

In a small interval for energy [0,5] A MeV, the largest Lyapunov exponent increases rapidly and within the next range of [5,30] A MeV is characterized by a slightly smaller slope. From $E = 30$ A MeV, the exponent decreases and after a small fluctuation, taking place at about 150 A MeV, it decreases again up to a global, almost vanishing, minimum at an energy of about 500 A MeV. Further on the curve is monotonically increasing up to 1400 A MeV, when a plateau is reached. The behavior of the largest Lyapunov exponent is fully consistent with the properties revealed by the Poincaré surface of sections. In this context one may say

that the largest Lyapunov exponent reflects to what extent the volumes of different resonances overlap with each other.

We recall that the results presented above correspond to a relatively large value for B. For a smaller $B(\leq 0.4$ A MeV), one finds a different energy dependence of both the Poincaré surface of sections and the largest Lyapunov exponent. Indeed, in this case the slope for the largest Lyapunov exponent is smaller and the phase space will never be dominantly chaotic. In this respect, the behavior of the largest Lyapunov exponent (as a function of energy) resembles that corresponding to the case of $B = 0.55$ and $E \geq 600$ A MeV, i.e. widespread chaos is slowly developing. If B is smaller, the widespread chaos cannot develop at all. Therefore, irrespective of the energy value, the phase space is filled with tori due to the dominant effect of the integrable Hamiltonian. Of course for low and high energies the dominance is generated by different terms of H_0.

Before concluding we note that the largest Lyapunov exponent has the inverse time dimension. Therefore one might think that by changing the energy, the time-scale is changed and therefore the results obtained for different energies cannot be compared with each other. As can be easily understood from our previous comments the unit for λ is $\frac{A}{\hbar}$ which is kept constant for all energies considered here. The agreement between the Lyapunov exponent behavior, as a function of energy, and the change in the Poincaré surface section is remarkable. To give an example, the minimum at $E \approx 400$ A (MeV) for λ (see Fig. 1(h)) indicates that for this energy the motion is regular which is alternatively shown in Fig. 1(e) by the Poincaré surface of section.

In conclusion, we have analyzed a Hamiltonian system exhibiting an important regular phase space volume, although not always dominant, for any energy. This behavior is determined by the fact that the H_1 term, making the system non-integrable, is not of the largest power in coordinates, among the terms defining the potential energy.

4. Chaotic Features of the Boson Hamiltonian H_B

The boson Hamiltonian H_B was obtained through quantization procedure from the classical energy function $\mathcal{H}$ given by (2.8). Reversely, the classical energy function can be obtained from H_B by a dequantization operation consisting of averaging H_B on a coherent function:

$$\phi = \exp\left[z_0 a_0^\dagger + z_2 a_2^\dagger - z_0^* a_0 - z_2^* a_2\right] |\, 0\,\rangle' \tag{4.1}$$

where $|0\rangle'$ stands for the vacuum state of the boson operators $a_0^\dagger$, $a_2^\dagger$, a_0, a_2.

Due to this relationship between H_B and $\mathcal{H}$ one expect a certain connection between the relative volume occupied by the chaotic trajectories and the spacing distribution for the eigenvalues of H_B. In order to investigate the correspondent

features from the two representations, one needs the eigenvalues of H_B. These have been found through a diagonalization procedure by using the basis:

$$|n_1 n_2\rangle = \frac{1}{\sqrt{n_1! n_2!}} (a_0^\dagger)^{n_1} (a_2^\dagger)^{n_2} |0\rangle' . \tag{4.2}$$

The cases $B \neq 0$ and $B = 0$ were separately studied. 1250 vector states have been considered. However we kept only those eigenvalues which do not vary by more than 5 per cent of the average energy spacing when the diagonalization basis is enlarged. This property is fulfilled only by 200-250 eigenvalues. The Hamiltonian H_B with $B \neq 0$ admits C_{3v} as symmetry group. Therefore, its eigenvectors can be classified by the irreducible representations (*irrep*) of this group. It is well known that C_{3v} has three *irreps*: one is two-dimensional while the remaining two are one-dimensional. The states belonging to these representations are double degenerate, symmetrical (against the reflexion operation $a_0 \to a_0$, $a_2 \to -a_2$) and anti-symmetrical, respectively. The level spacing distribution was calculated first for each irreducible representation and then the results summed up. In the energy interval of [0, 35] A (MeV), for a given value of B lying in the interval [0, 0.6] A (MeV), one has found a number of 30–50 energy levels. The later interval was covered by changing B with a step of 0.025 A (MeV). This seems to be the minimum length for the energy distance of two consecutive B's producing independent distributions. For each value of B the mean-level spacing was determined for the energy interval mentioned above. In all figures shown in the present paper, the energy spacing between two consecutive levels (alternatively called nearest neighbor spacing) are considered in units of the mean energy spacing. The probability of having a spacing in the interval $[S, S + \Delta S]$ is given by the quantity $P(S)\Delta S$. For illustration, in Fig. 2, we present the results obtained by summing the spacing distributions of states corresponding to the three representations, for the following values of B: 0.1 A, 0.2 A, 0.3 A, 0.4 A, 0.5 A, 0.6 A (MeV). Any of these curves corresponds to a statistic of 200–250 levels (some of them are double degenerate). Note that for small (0.1 A) and large (0.5 A, 0.6 A) values of B the most likely spacing is equal to about one. This means that despite then presence of the third and fourth order anharmonic terms, the harmonic term, producing the equidistant spectrum, prevails. Also it is worth mentioning that for $B \geq 0.4$ the predicted curves resemble the Wigner distribution. This reflects the fact that in these ranges of B and E, the classical motion is dominantly chaotic, as shown in Fig. 1(h). In contrast, for $B < 0.4$ A MeV the phase space is mainly occupied by regular orbits.

Of course, in order to draw definite conclusions better statistics would be desirable. Since $B < 0.4$ A MeV and $B \geq 0.4$ A MeV are classically distinguished by the way chaos is developed in the energy range of [0, 35] A MeV, whereas for two values of B belonging to one of the two ranges chaos similarly depends on the system energy, a solution for improving the level spacing statistics would be to sum the distributions corresponding to different B's, with a spacing of 0.025 A MeV,

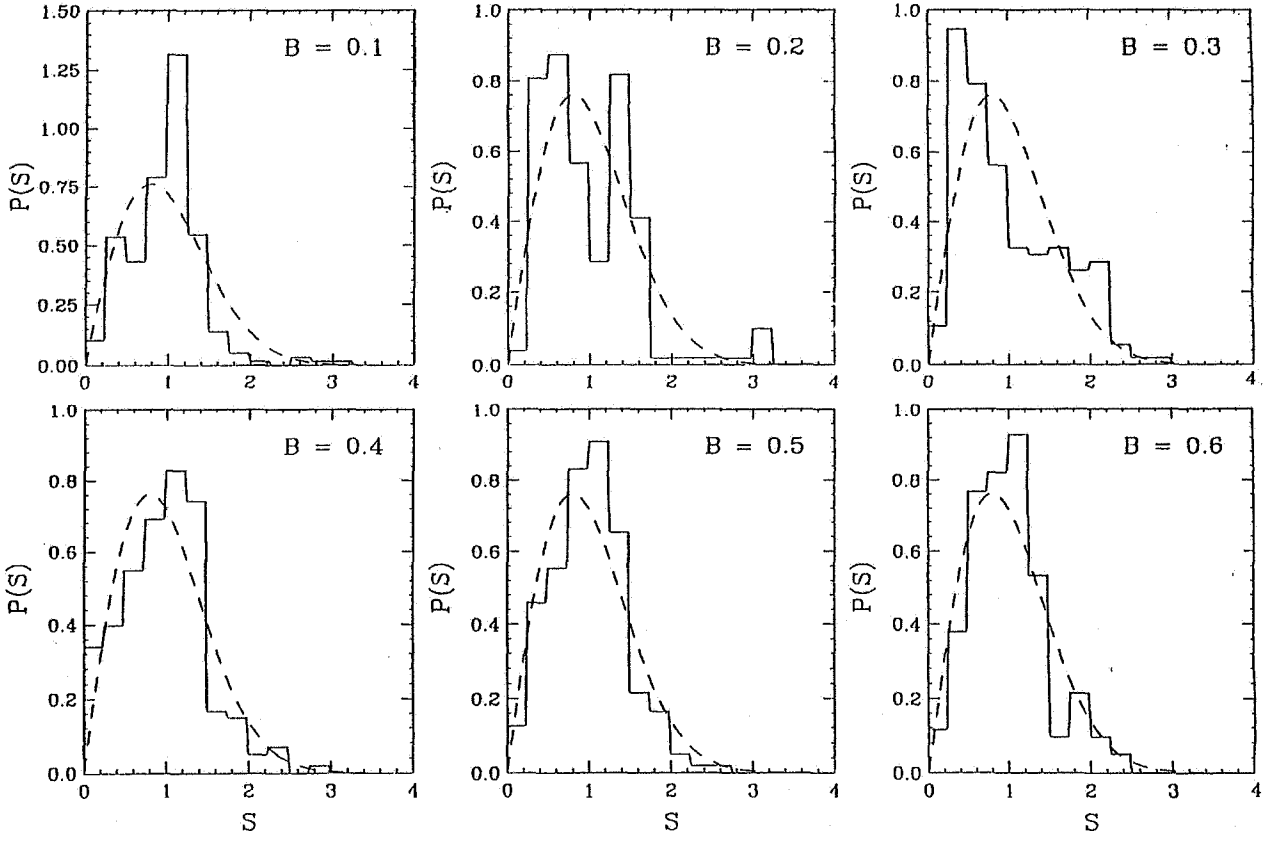

Fig. 2. The probability distributions for energies corresponding to the values of B: 0.1 A, 0.2 A, 0.3 A, 0.4 A, 0.5 A, 0.6 A(MeV). The curves are obtained by summing the histograms corresponding to the three irreducible representations of C_{3v}.

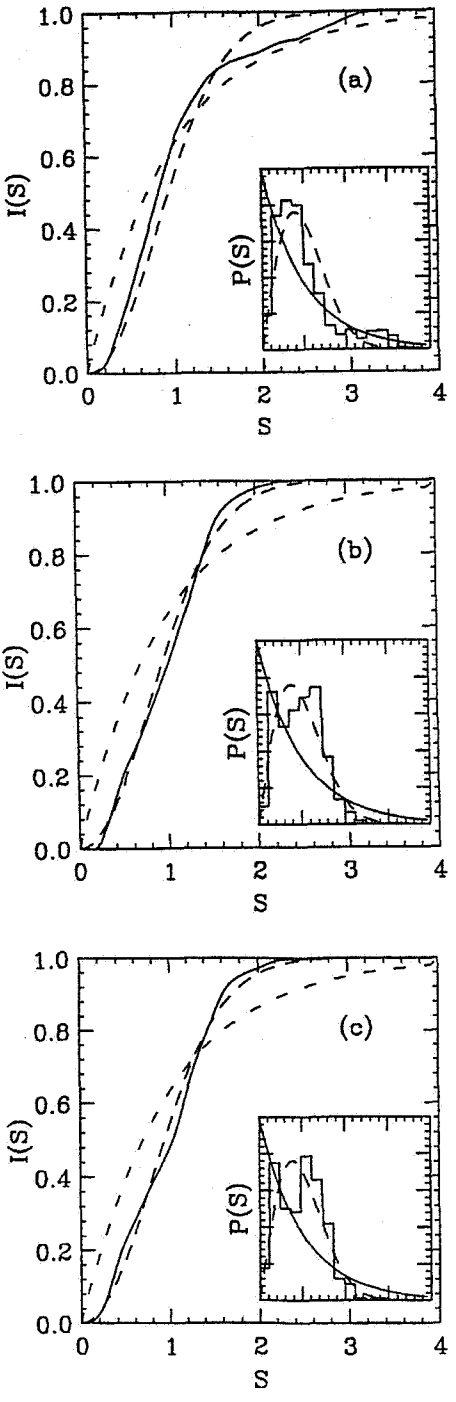

Fig. 3. Probability distribution for energy levels corresponding to the three irreps of C_3v (a) bidimensional (b) symmetrical one-dimensional and (c) anti-symmetrical one-dimensional. The result is obtained by summing all distributions corresponding to $B < 0.4$ A (MeV). For each case the cumulative probability distribution $I(S)$ (full line) is compared with those corresponding to the Wigner (long dash line) and poisson (dash line) distributions.

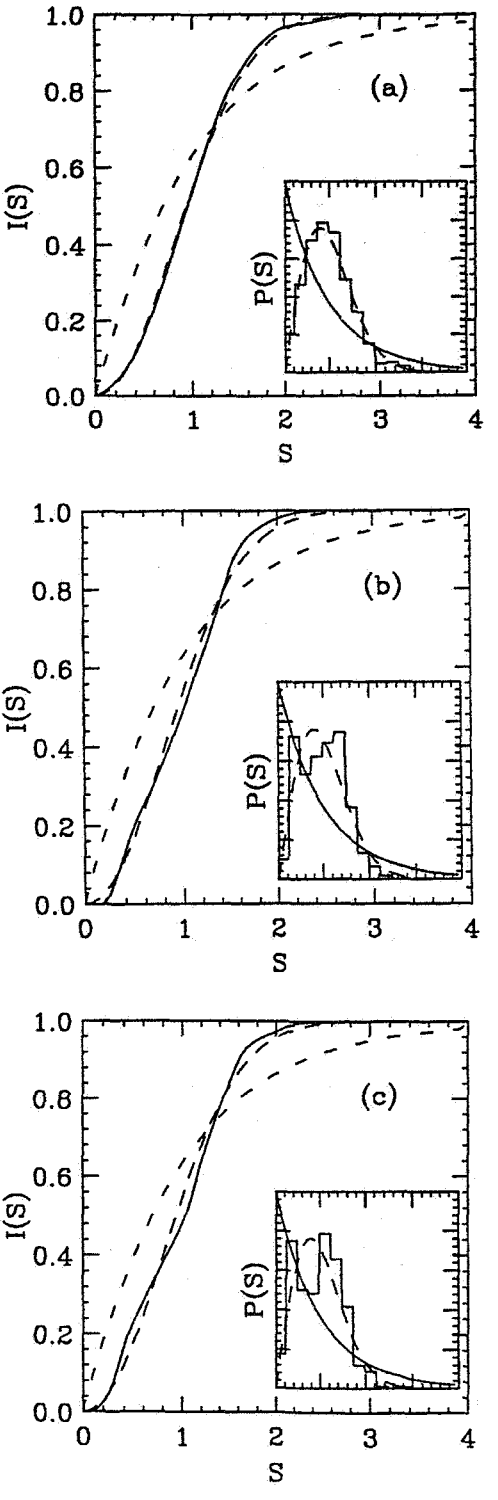

Fig. 4. The same as in Fig. 3 but for 0.4 A $\leq B \leq$ 0.6 A (MeV).

from each interval. The results are plotted in Figs. 3 and 4 for the intervals $B <$ 0.4 A MeV and $B \geq 0.4$ A MeV, respectively. The three irreps of the C_{3v} group were separately considered. For each case the cumulative spacing distribution $I(S)$ (i.e. the probability to find spacing smaller than S) is plotted as a function of the level spacing S, taken in units of mean-level spacing. For $B < 0.4$, spacing distributions exhibit large deviations from the Wigner one. Indeed, they seem to intermediate the Wigner and Poisson distributions. The states belonging to the two-dimensional C_{3v} representations deviate more substantially from the Wigner distribution while for one-dimensional representations deviations are smaller. These features are seen from the spacing distribution curves ($P(S)$) but much more clearly from the curves for the cumulative distribution $I(S)$. For $B \geq 0.4$ A MeV, the agreement with the Wigner distribution is very much improved. This is caused by the energy interval [0, 35 A] (MeV) and the phase space is dominantly filled up with chaotic trajectories. Summing the distributions in the two intervals of B, corresponding to the states from the same *irrep*, one obtains the results shown in Figs. 5(a), (b) and (c), respectively. We remark that the agreement with the Wigner distribution is improved, especially for the asymmetrical one-dimensional representation. The result of summing the distributions from Fig. 5 is plotted in Fig. 6 a where quite a good agreement with the Wigner distribution is obtained. This is also illustrated in Fig. 6(b) where the cumulative distribution of the level spacings is plotted.

Let us turn our attention now to the $B = 0$ case. In Ref. 37 we have proved that for $B = 0$ the classical equations of motion are integrable and the two constants of motion were explicitly given. Operators a_0^+, a_0, a_2^+, a_2 may be used to define a rotation group $\mathfrak{R}_3$, characterized by the generators:

$$T_x = \frac{1}{2}(a_2^+ a_2 - a_0^+ a_0)\,, \quad T_y = \frac{1}{2}(a_0^+ a_2 + a_2^+ a_0)\,, \quad T_z = \frac{1}{2i}(a_0^+ a_2 - a_2^+ a_0)\,. \tag{4.3}$$

By direct calculation one checks that H_B is invariant with respect to rotations around the z-axis, i.e.

$$[H_B, T_z] = 0\,. \tag{4.4}$$

Another symmetry invariance of H_B is given by the permutation

$$(a_0^\dagger, a_0) \leftrightarrow (a_2^\dagger, a_2)\,. \tag{4.5}$$

Therefore the eigenstates of H_B are either symmetrical or anti-symmetrical against the permutation operation defined by Eq. (4.5). Moreover, the eigenvalues are double degenerate. Degenerate states have equal magnitudes but different signs for the eigenvalue of T_z, t_z. This reflects, in fact, that T_z changes its sign against the permutation transformation 4.5. Of course there are non-degenerate states characterized by a vanishing value for t_z. The results for the case $B = 0$ are given in Fig. 6(c). There, the result of summing the distributions obtained for symmetric and asymmetric states respectively, is shown. One notes large deviations from Poisson distribution for both the $P(S)$ and $I(S)$ functions.

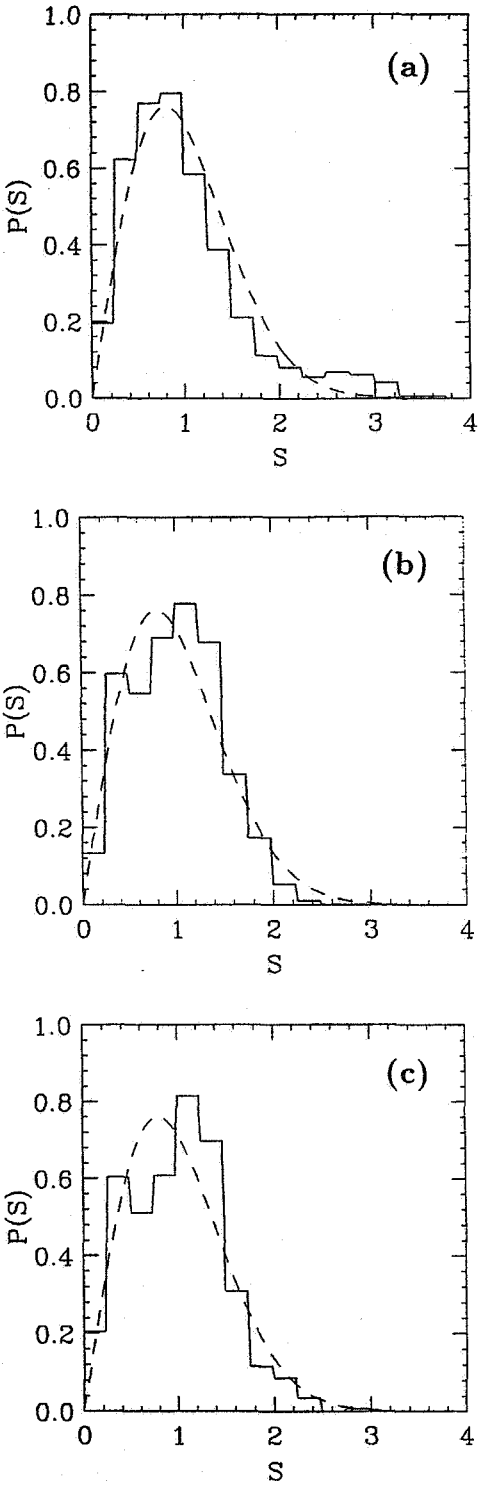

Fig. 5. The same as in Fig. 3 but for 0.1 A $\leq B \leq$ 0.6 A (MeV).

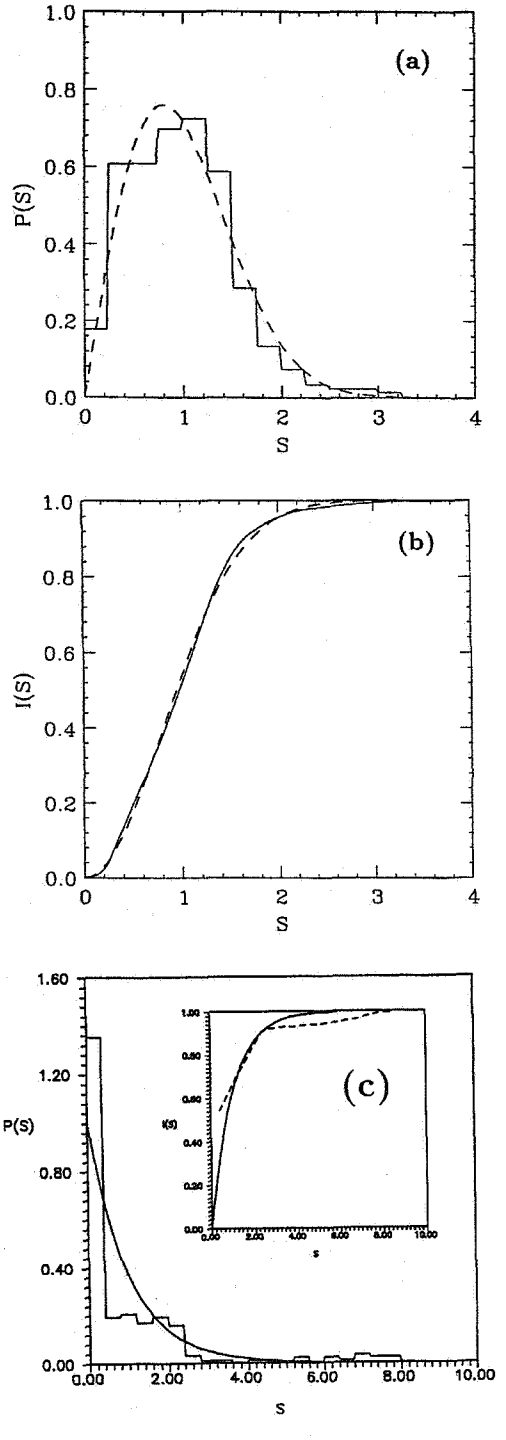

Fig. 6. (a) Probability distribution for energy levels obtained by summing the distributions from Fig. 5. (b) The cumulative probability distribution $I(S)$ for the present calculations (full line) as well as for the Wigner distribution (dash line) are also given. (c) Probability distribution for energy levels, $P(S)$, and cumulative distribution, $I(S)$, are presented for the case of $B = 0$.

In what follows we would like to comment on possible reasons for these deviations. Suppose that the fourth order term is missing. The remaining Hamiltonian is a plane oscillator with equal frequencies on the "x" and "y" directions. In such a case,according to Ref. 47, the nearest neighbor spacings distribution goes to infinity when the spacing approaches zero. As a matter of fact this may explain the non-generic feature obtained for the situation when $B \neq 0$. Indeed, switching on the fourth order term the plane oscillator degeneracy is only partially removed. Indeed a double degeneracy still persists and this would not exist if the two oscillators had different frequencies. The double degeneracy of some states causes an over-accumulation of the spacing probability in $S = 0$. Consequently, a discontinuity of this function does appear:

$$\lim_{\epsilon \to 0} P(\epsilon) \neq P(0)\,. \tag{4.6}$$

This discontinuity leads to a cumulative distribution, defined as the area of the surface bordered by the $P(S)$ histogram, different from zero in $S = 0$. To conclude this analysis for low values of S, the cumulative distribution exceeds the Poisson distribution since the Hamiltonian H_B involves a plane oscillator with equal frequencies along the "x" and "y" axes. The predicted cumulative distribution is very close to the cumulative Poisson distribution in the interval [1, 2.8] of S. Since the mean spacing is quite small (0.3 MeV), there are non-vanishing histograms for relatively large values of S due to the large number of degenerate states. Despite this feature, the predictions lie below the cumulative Poisson distribution in a large interval [2.8, 8.2]. Also, it is worth mentioning that there are three windows with about equal lengths (≈ 0.15) and starting in $S = 3.8$, 4.8, 5.8 respectively, which do not comprise any spacing. It is interesting to check whether the global behavior obtained in Fig. 6(c) is also a signature for the states with given t_z. We did this for the states with $t_z = 0$ and got a negative answer. Indeed, the NNS distribution looks like a narrow bell centered on $S = 1$. This means that the anharmonic term of fourth order in coordinates does not affect these states significantly and consequently the harmonic features prevail.

In conclusion, the case of $B = 0$ is characterized by NNS distribution exhibiting large deviations from the Poisson one for both small (≤ 1) and large (≥ 2.8) spacings. Similar conclusions were earlier obtained by Brack *et al.*[50] for Henon–Heils potential.

In this paper we investigated the classical and quantal properties of the intrinsic degrees of freedom, q_0 and q_2, which can be related to the nuclear deformations β and γ.[37] On top of each state, obtained by diagonalizing H_B, one may construct a full rotational band whose states are eigenvectors of the starting model Hamiltonian H (2.1). The rotational energies added to the intrinsic state energies differ from each other since they are determined by different moments of inertia. Hence, the statistics for states of a given angular momentum is expected to be different from that obtained here for the eigenvalues of H_B. As shown in Ref. 18 some of them $(2^+, 4^+)$ satisfy the Poisson statistics and others deviate substantially from this

distribution. The connection between the statistics satisfied by the eigenvalues of H_B and that which characterize the energy levels of H (2.1) will be treated in a forthcoming paper.

Another point which we want to touch on concerns the apparently unphysical energy interval where the NNS plots are presented. In this context it is worth mentioning the heavy ion reactions where part of the colliding energy is distributed to the surface degrees of freedom describing the prepared hot nuclei. The nonlinear description of the system evolution requires the inclusion of 20 to 30 phonon states lying in the energy range considered here. The thermal motion of nuclear surface is usually described by Langevin type equations. Our paper suggests that such a study can also be performed with the Hamilton equations which exhibit the advantage of having a quantal counterpart description, showing the statistical properties of the thermal motion of nuclear surface. Since the thermal motion at higher energies become chaotic, the coupling of nuclear hot surface motion and the giant resonance, or other types of collective motion at high energy, might generate interesting phenomena related to the global motion character.

5. Conclusions

In previous sections we studied a quadrupole boson Hamiltonian at both the semiclassical and quantum mechanical levels. For this model Hamiltonian, which is very often used to describe the spectroscopic properties of medium and heavy nuclei, we endeavored to check, by means of a careful numerical analysis, whether a chaotic/regular classical motion determine a chaotic/regular quantal spectrum as it was stated by Percival in Ref. 6.

Although the classical behavior was studied in a previous publication,[37] here we consider it again but for higher energies. The interesting result obtained in this paper contrasts with the previous known ones, stating that the chaoticity of a system increases with energy. Indeed, since the regular part of the Hamiltonian comprises the fourth power in coordinates, by increasing the energy the relative effect coming from the third order term is diminished, resulting in an expanding volume for the regular trajectories. The quantal spectrum is analyzed in the interval [0, 35] A MeV by calculating the nearest neighbor spacings distribution as well as the cumulative distribution. The transition from the regular ($B = 0$) to chaotic ($B \geq 0.4$ A MeV) spectrum, revealed that the spacing distributions goes from a Poisson-like to a Wigner shape is fully consistent with the classical picture shown by Poincaré surface of sections and largest Lyapunov exponents.

One may ask whether by increasing the diagonalization space (and by this the energy of the considered levels) for this particular Hamiltonian, the Wigner distribution will go back to a Poisson-like distribution. The answer to this question is however implicitly given by the ergodic hypothesis, which is commonly accepted in such analysis. Indeed, since for $E \geq 600$ A (MeV) and $B = 0.55$ A (MeV) the classical phase space exhibits a similar structure, concerning the distribution

of chaos, with that associated to $B \leq 0.4$ A (MeV). At lower smaller energies, one expects that the two energy intervals are characterized by similar NNS distributions. Deviations from this picture can be investigated only by a careful numerical analysis. However this interesting feature requires tremendous additional computational work and moreover falls beyond the announced scope of the present paper.

Our paper raises a very difficult, but otherwise very important, principle: Suppose one reaches the conditions which allow the diagonalization of very large matrices so that the largest eigenvalues lie in the energy range studied in Fig. 1, showing the Poincaré sections. Within this interval, the dynamic oscillations from chaos to order and again to chaos. On the other hand the spacing distribution takes into account all eigenvalues provided by the diagonalization procedure. Of course for such a situation one cannot speak about a global correspondence between the classical features and the spectral distribution. In fact the "local" character for such a mapping is evident even for a relatively small energy interval such as that which was analyzed here.

Concerning the relevance of the present work in nuclear physics, we would like to comment on the following features:

a) The fundamental task of any many-body theory is to interpret the collective phenomena in terms of single particle motion. Thus, most of the specific features of the many-body collective motion are determined by the properties of the single particle mean field. Such a determinism is not, however, evident for chaotic motion. Indeed, it is not rigorously proven that the chaotic features of the motion of a single particle in deformed potentials are really the reason for the GOE type fluctuations in the quantum spectra of the nuclear many-body problem. Due to this fact many efforts have been made to study both the single particle motion in various deformed potentials and the collective motion. We should mention that our work is also devoted to this aim.

b) Long time ago, Moszkowski proposed a schematic model to study an interacting many-body system moving in a plane. The interaction consists of a spin-orbit and a quadrupole-quadrupole term.[51] Such a model is able to describe in a unified fashion the single particle and collective features[52] of the nucleon system. It is remarkable that the collectives variable, derived there, satisfy an equation which resembles the eigenvalue equation for the operator H_B given by (2.17). One might say that indeed the phenomenological Hamiltonian H_B can be derived from a many-body Hamiltonian. This remark allows us to assert that conclusions drawn here are also valid for the many-body collective motion.

c) The NNS analysis of collective states $2^+, 3^+, 4^+, \ldots$, etc. reflects a global behavior and one cannot say to what extent the chaotic behavior is due to the rotational motion or to the internal motion. In this regard it is worth saying again that our approach describes the motion of intrinsic degrees of freedom and by this performs one step forward to answering the above mentioned question.

d) As we have already mentioned, the results of the present paper might be useful for the description of statistical properties in hot nuclei.

References

1. A. N. Kolmogorov, *Dokl. Akad. Nauk. SSSR* **98** (1954) 527; V. I. Arnol'd, *Usp. Mat. Nauk.* **18**, No. 6 (1963) 91; J. Moser, *Stable and Random Motions in Dynamical Systems* (Princeton University Press, Princeton, 1973).
2. B. Chirikov, *Physics Reports* **52** (1979) 263.
3. G. H. Walker and J. Ford, *Phys. Rev.* **188** (1969) 416.
4. Wei-Min Zhang, Craig C. Martens, Da Hsuan Feng, and Jian-Min Yuan, *Phys. Rev. Lett.* **61** (1988) 216.
5. Y. Alhassid and N. Whelan, *Phys. Rev.* **C43** (1991) 2637.
6. I. C. Percival, *J. Phys. B, At. Mol. Phys.* **6L** (1973) 229–32.
7. M. V. Berry, *J. Phys. A: Math. Gen.* **10** (1977) 2083.
8. M. C. Gutzwiller, *J. Math. Phys.* **11** (1970) 1791; **12** (1971) 343, *Chaos in Classical and Quantum Mechanics* (Springer-Verlag, New York, 1990).
9. T. A. Brody, J. Flores, J. B. French, P. A. Mello, A. Pandey, and S. S. M. Wong, *Rev. Mod. Phys.* **53** (1981) 385.
10. R. A. Pullen and A. R. Edmonds, *J. Phys. A: Math. Gen.* **14** (1981) L319..
11. O. Bohigas and M. J. Giannoni, in *Mathematical and Computational Methods in Nuclear Physics*, eds. Dehesa, J. M. Gomez and A. Polls (Springer-Verlag, Berlin, 1983), p. 1.
12. J. Zakrzewski, K. Dupret and D. Delande, *Phys. Rev. Lett.* **74** (1995) 522.
13. B. V. Chirikov and D. L. Shepelyansky, *Phys. Rev. Lett.*, **74** (1995) 518.
14. H. A. Weidenmüller, in *Nuclear Structure 1985*, eds. R. A. Broglia, G. Hagemann and B. Herskind (North-Holland, Amsterdam, 1985), p. 213.
15. A. Richter, *Nucl. Phys.* **A553** (1993) 417c.
16. O. Bohigas and H. A. Weidenmuller, *Ann. Rev. Nucl. Part. Phys.* **38** (1988) 421.
17. R. U. Haq, A. Pandey and O. Bohigas, *Phys. Rev. Lett.* **48** (1982) 1086.
18. A. Y. Abul-Magd and H. A. Weidenmuller, *Phys. Lett.* **B162** (1985) 223.
19. J. F. Schriner, Jr, G. E. Mitchell and T. von Egidy, *Z. Phys. A* **338** (1991) 309.
20. R. Arvieu, F. Brut, J. Carbonell, and J. Touchard, *Phys. Rev.* **A35** (1987) 2389.
21. J. Carbonell, F. Brut, R. Arvieu, and J. Touchard, *J. Phys.* **G11** (1995) 385.
22. R. Arvieu, P. Rozmej and M. Ploszajczak, in *New Trends in Theoretical and Experimental Nuclear Physics*, Proceedings of the Predeal International Summer School, 1991, World Scientific, eds. A. A. Raduta, D. S. Delion and I. I. Ursu, p. 232.
23. D. C. Meredith, S. E. Kooninand and M. R. Zirnbauer, *Phys. Rev.* **A37** (1988) 3499.
24. V. G. Soloviev, *Nucl. Phys.* **A554** (1993) 77.
25. V. G. Soloviev, *Nucl. Phys.* **A586** (1995) 265.
26. W. D. Heiss, R. G. Nazmitdinov and S. Radu, Phys. Rev. Lett. **72** (1994) 2351.
27. W. D. Heiss, R. G. Nazmitdinov and S. Radu, *Phys. Rev.* **B51** (1995) 1874.
28. D. Biswas, S. Pal and A. Chaudhuri, *Phys. Rev.* **A46** (1992) 6817.
29. V. Paar and D. Vorkapic, *Phys. Lett.* **B205** (1988) 7.
30. V. Paar and D. Vorkapic, *Phys. Rev.* **C41** (1990) 2397.
31. Y. Alhassid, A. Novoselsky and N. Whelan, *Phys. Rev. Lett.* **65** (1990) 2971.
32. Y. Bolotin, V. Y. Gonchar and E. V. Inopin, *Yad. Fiz.* **45** (1987) 350.
33. V. Paar, D. Vorkapic and K. Heyde, *Phys. Lett.* **B211** (1988) 265.
34. H. Seyfart, S. Brant, P. Gottel, V. Paar, D. Vorkapic, and D. Vretenar, *Z. Physik A-Atomic Nuclei* **330** (1988) 141.
35. V. Lopac, S. Brant and V. Paar, *Z. Phys. A-Atomic Nuclei* **337** (1990) 131.
36. F. J. Dyson and M. L. Mehta, *J. Math. Phys.* **4** (1963) 701.
37. V. Baran, A. A. Raduta and D. S. Delion, *Phys. Rev.* **E54** (1996) 3264.
38. A. A. Raduta, V. Baran and D. S. Delion, *Nucl. Phys.* **A588** (1995) 431.

39. G. Gneuss, U. Mosel and W. Greiner, *Phys. Lett.* **30B** (1969) 397; M. Seiwert, P. O. Hess, J. A. Maruhn, and W. Greiner, *Phys. Rev.* **C23** (1981) 2335; P. O. Hess, J. Maruhn and W. Greiner, UFTP, preprint Frankfurt/Main, 8 (1980).
40. S. G. Lie and G. Holzwarth, *Phys. Rev.* **C12** (1975) 1035.
41. M. Henon, "Numerical exploration of Hamiltonian systems", in *Chaotic Behavior of Deterministic Systems*, Les Houches 1981, eds. G. Iooss, R. H. G. Helleman and R. Stora (North-Holland, Amsterdam, 1982), p. 53; M. Henon and C. Heiles, *Astron. J.* **69** (1964) 73.
42. A. Bohr, *Mat. Fys. Medd. Dan. Vid. Selsk.* **26**, no. 14 (1952); A. Bohr and B. Mottelson, *ibid.* **27**, no. 16 (1953).
43. W. Greinerand and J. M. Eisenberg, *Nuclear Theory, vol. I, Nuclear Models*, p. 377.
44. W. H. Steeb and J. A. Louw, *Chaos and Quantum Chaos* (World Scientific, Singapore, 1986).
45. G. Benettin, L. Galgani and J. M. Strelcyn, *Phys. Rev.* **A14** (1976) 2338.
46. M. Henon, "Numerical exploration of Hamiltonian systems", in *Chaotic Behavior of Deterministic Systems*, Les Houches 1981, eds. G. Iooss, R. H. G. Helleman and R. Stora (North-Holland, Amsterdam, 1982), p. 122.
47. M. Berry, in *Chaotic Behavior of the Deterministic Systems*, Les Houches 1981, eds. J. Joss, R. H. G. Helleman and R. Stora (North-Holland, Amsterdam, 1982), p. 173.
48. V. I. Oseledec, *Trans. Mosc. Math. Soc.* **19** (1968) 197.
49. L. E. Reichl, *The Transition to Chaos in Conservative Classical Systems: Quantum Manifestations* (Springer-Verlag, New York, 1992), p. 43.
50. M. Brack, R. K. Bhaduri, J. Law, M. V. N. Murthy and Ch. Maier, *Chaos* **5** (1995) 707.
51. S. A. Moszkowski, *Phys. Rev.* **110** (1958) 403.
52. A. A. Raduta, *Phys. Rev.* **C51** (1995) 2973.